Psychol Res (1996) 58: 254–273

ORIGINAL ARTICLE

Jonathan Vaughan · David A. Rosenbaum · Frederick J. Diedrich · Cathleen M. Moore

Cooperative selection of movements: The Optimal Selection model

Received: 4 January 1995 / Accepted: 5 July 1995

Abstract How one selects a movement when faced with alternative ways of doing a task is a central problem in human motor control. Moving the fingertip a short distance can be achieved with any of an infinite number of combinations of knuckle, wrist, elbow, shoulder, and hip movements. The question therefore arises: how is a unique combination chosen? In our model, choice is achieved by consideration of the similarity between the task requirements and the optimal biomechanical performance of each limb segment. Two variants of the model account for the movements that are selected when subjects freely oscillate the fingertip and when they tap against an obstacle. An important feature of both is that the impulse of collision with an obstacle (as in drumming with the hand or tapping with the finger) is assumed to be controlled in part by aiming for a point beyond the surface being struck. Thus, a force-related control variable may be represented and controlled spatially.

Introduction

Despite the resurgence of interest in motor control in the last few decades, it has become increasingly clear that current approaches may not provide adequate means of addressing some of the fundamental aims of research in this area. For example, one of the central unanswered questions is how people select an appropriate mode of action when there are a number of roughly equivalent alternatives; this is often referred to as the "degrees of freedom" problem (Bernstein, 1967). The problem arises from the fact that there are usually an infinite number of ways of achieving a task such as placing the fingertip at a particular location in three-dimensional space. While some work has been done on the degrees-of-freedom problem in the selection of movement patterns for single moving points, such as the hand during aiming (Hogan & Flash, 1987; Meyer, Abrams, Kornblum, Wright, & Smith, 1988), very little work has been done on the means by which entire limb-segment patterns are coordinated. In the present paper, we address this problem by considering the ostensibly simple task of moving the fingertip from one location to another a few centimeters away. Any of an infinite number of combinations of knuckle, wrist, elbow, and shoulder movements can achieve the task. Yet a single combination must be chosen. How is the choice made?

The research presented here leads us to advocate a model in which each segment is represented independently, and the selection of a particular movement pattern results from the simultaneous activation of each representation. Because the model characterizes movement selection as a cooperative process that occurs for all segments simultaneously, it accords with recent developments in connectionist approaches to cognitive psychology, which seek to avoid a homunculus or omniscient executive (Rumelhart & McClelland, 1986). Furthermore, because the model is grounded in biomechanics and in considerations of energy efficiency, it serves to unite biomechanical approaches to motor control with cognitive approaches. Finally, the model can plan without having to compute a full analysis of the dynamics of each segment's movements of its interactions with neighboring segments.

The underlying principles of the model were recently presented by Rosenbaum, Slotta, Vaughan, and Plamondon (1991) in connection with a task in which

J. Vaughan (✉)
Department of Psychology, Hamilton College, 198 College Hill Road, Clinton, NY 13323, U. S. A.

D. A. Rosenbaum
Department of Psychology, Penn State University, U. S. A.

F. J. Diedrich · C. M. Moore
Department of Psychology, Hamilton College, U. S. A.

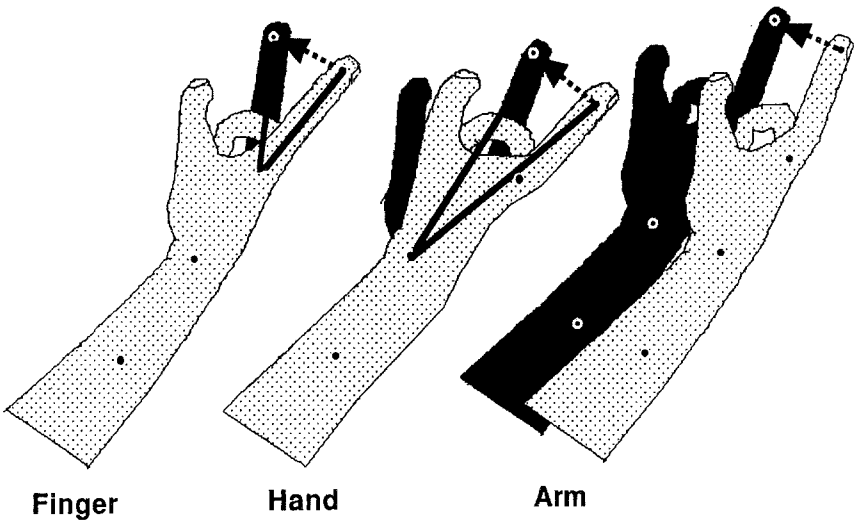

Fig. 1 Equivalent displacement of the fingertip achieved entirely by finger (left), hand (center), and arm movement (right)

subjects could translate the fingertip along a horizontal fronto-parallel axis in an infinite number of ways – by moving the finger via flexion or extension of the first metacarpophalangeal joint, by moving the hand via flexion or extension of the wrist, by rotating the forearm via flexion or extension of the elbow, or by any combination of these methods (see Figure 1). The independent variables in the experiment were the distance to be covered and the frequency of back-and-forth fingertip displacements. The model's central concept was that the relative contributions of the individual limb segments to fingertip displacement would depend on each segment's fit to the task demands, which depends in turn on that segment's optimal frequency and amplitude.

Evaluation of the model required an initial determination of the optimal performance characteristics of each segment (the finger, the hand, or the arm) when it is used in isolation. Minimal effort is assumed to define a particular amplitude at each frequency, and a particular frequency at each amplitude, that is most efficient. To measure these optimal performance characteristics, subjects were asked to oscillate the fingertip using one segment (only the finger, the hand, or the arm) in the "most comfortable" manner at each of several required frequencies (with amplitude free to vary), and at each of several required amplitudes (with frequency free to vary). While each segment was being used, the subject held the other segments still.

The optimal amplitude of fingertip displacement and the optimal frequency of oscillation differed depending on which segment was used. The optimal frequency of the forearm was lower than that of the hand, which was lower than that of the finger. Conversely, the optimal amplitude of the forearm (expressed in terms of the resulting displacement of the fingertip) was larger than that of the hand, which was larger than that of the finger. In addition, the amplitude that was produced changed within each segment as the required frequency of oscillation was varied. For all three segments, larger amplitudes of oscillation were produced at slower oscillation frequencies.

To observe how subjects performed multijoint movements, the same subjects were asked, in the second part of the experiment, to oscillate the fingertip at each of the possible combinations of the optimal amplitudes and frequencies that had been observed in Experiment 1, using whatever combination of finger, hand, and arm they wished. Rosenbaum et al. (1991) found that the limb-segment combinations spontaneously selected varied with the frequency and amplitude required in each condition, and that each segment contributed most when the required amplitude and frequency came closest to its optimal values.

To account for the changes in the involvement of individual limb segments, Rosenbaum et al. (1991) developed the Optimal Selection model, according to which, when a task is presented, each effector's ability to perform the task is evaluated with respect to its optimal performance when it acts alone. In tasks that allow more than one segment to contribute, each segment (or its corresponding module) evaluates its own effectiveness for completing the task. Weights are assigned to the effectors based on their relative evaluations. Thus, when a particular amplitude and frequency of fingertip oscillation are required, the closer that task comes to each segment's optimal amplitude and frequency, the higher the weight assigned to that segment. The relative contributions of the effectors that are observed are assumed to reflect the weights that are assigned.

The Optimal Selection model accounted qualitatively for the data of Rosenbaum et al. (1991). Each segment contributed the most when the task requirement matched its own optimal frequency and amplitude. However, the model was not fitted quantitatively

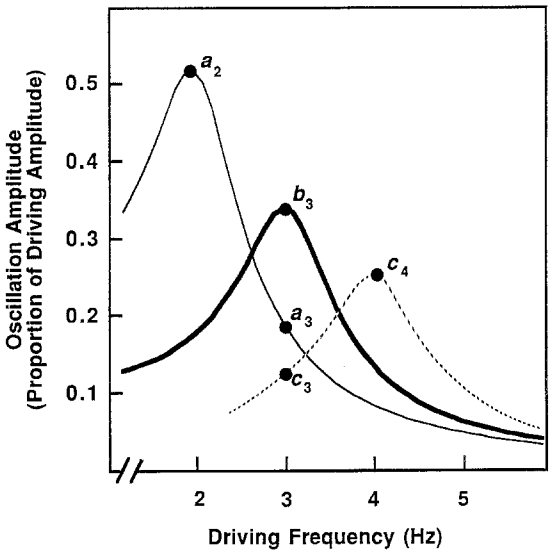

Fig. 2 Hypothetical frequency-amplitude functions for three systems of equal mass and driving force, each having a different resonant frequency as a consequence of a different stiffness. (The three curves represent oscillators having resonant frequencies of 2 Hz, 3 Hz, and 4 Hz, for which points a_2, b_3 and c_4, respectively represent the maximum amplitude produced by a constant driving force at that system's resonant frequency. For comparison with point b_3 [the amplitude produced in system b, which has a resonant frequency of 3 Hz, by a driving force of 3 Hz], point a_3 represents the amplitude produced in system a [which has a resonant frequency of 2 Hz], by the 3-Hz driving force, and point c_3 is the amplitude produced in system c [which has a resonant frequency of 4 Hz] by the same 3-Hz driving force.)

to the data. One aim of the present study was to provide such a quantitative fit. A second aim was to explore the underlying basis of the optimal performance functions that characterized the three limb segments. Thus, we sought to explain why the optimal frequencies and amplitudes of the finger, the hand, and the arm were ordered as they were. A third aim was to extend the Optimal Selection model to a new, but related, task – oscillating the fingertip to produce controlled collisions with an obstacle. This task is analogous to drumming or finger-tapping. Finger-tapping has been widely used in studies of human timing and rhythmic performance (for reviews, see Wing, 1980; Rosenbaum, 1991, Chapter 8). From such studies, detailed models of internal timing mechanisms have been developed (Collard & Povel, 1982; Rosenbaum, Kenny, & Derr, 1983; Summers, Rosenbaum, Burns, & Ford, 1993; Vorberg & Hambuch, 1978; Wing, 1980). It is surprising, given the strong interest in finger-tapping, that little research has been done on the movements made during tapping performance. Thus, independently of the model developed here, the description of such movements in terms of the kinematics of the fingertip and the contributions of the limb segments may prove useful for future investigations.

The basis for optimal amplitudes and frequencies

What was the basis of the optimal frequencies and amplitudes observed by Rosenbaum et al. (1991)? Why were amplitude and frequency reciprocally related for each limb segment, and why were the optimal frequencies of oscillation and the optimal angular amplitudes smaller for the forearm than for the hand and smaller for the hand than for the finger?

We propose that the differences in optimal frequencies and amplitudes resulted from two biomechanical factors – energy efficiency and modulation of joint stiffness. Our proposal is closely related to proposals in biomechanics concerning, for example, the control of walking rate. Spontaneously selected walking rates usually correspond to rates that can be shown to minimize energy expenditure (Holt, Hamill, & Andres, 1991). We propose that subjects in finger-waving and finger-tapping tasks likewise try to minimize energy when satisfying overt task demands, by simultaneously selecting effectors and adjusting their stiffnesses so that the limb's resonant frequency, ω_0, matches the task (driving) frequency, ω_r.

If the segment's resonant frequency were higher or lower than the driving frequency, a smaller amplitude of oscillation would be produced by a constant-amplitude driving force. For example, a driving frequency of 3 Hz produces a smaller amplitude for an oscillator of resonant frequency 2 or 4 Hz (as shown by points a_3 and c_3 in Figure 2) than it does for an oscillator of resonant frequency 3 Hz. Thus, if the resonant frequency of each limb segment were fixed, one way to achieve efficient performance (the greatest amplitude for a constant driving force) would be to use the segment whose resonant frequency most closely matches the driving frequency.

The resonant frequency of a segment is not fixed, however. It can be varied by the modulation of joint stiffness, which in turn can be controlled by the variation of the co-contraction of the muscle groups acting on the segment (Hasan, 1986). Thus, another way of achieving efficient performance is to adjust the resonant frequency of one or more segments to match the driving frequency, so that they resonate at the required frequency.

In this manner, we can explain the finding of Rosenbaum et al. (1991) that the amplitude produced by each segment acting alone decreased as its required oscillation frequency increased. Assuming that the limb segment was stiffened as ω_r increased, so that the segment could always perform at a corresponding ω_0, the maximum amplitude produced at each frequency for a constant driving force would decrease accordingly. A decline in amplitude with required frequency has also been reported for alternating flexion and extension of the wrist alone by Kay, Kelso, Saltzman, and Schöner (1987). Kay et al. analyzed this relationship in terms of the dynamics of oscillation of the wrist, which they

characterized with a hybrid oscillation model that combined the characteristics of a harmonic (van der Pol) oscillator and a Rayleigh oscillator. The hybrid oscillator accounted for the linear relationship observed between the optimal amplitude of oscillation and the driving frequency in much the same way as is proposed here. Similarly, Feldman (1980) showed that there is an inverse relation between maximum amplitude of (elbow) angular displacement and oscillation frequency. In accord with our emphasis on stiffness changes, Feldman showed that the increase in frequency was accompanied by increasing tonic coactivation of antagonist muscles.

Why, in Rosenbaum et al. (1991), were the optimal frequencies of oscillation, as well as the optimal angular amplitudes, smaller for the forearm than for the hand and smaller for the hand than for the finger? The ordering of the performance characteristics of the three segments follows from their physical characteristics and from principles of harmonic oscillation. First, mechanical factors favor smaller angular oscillation of large segments because the amplitude of oscillation produced by a driving force of constant frequency and amplitude is inversely proportional to the mass of the oscillated segment (see, e.g. Feynman, Leighton, & Sands, 1963). Second, harmonic oscillation favors faster oscillation in smaller segments because the resonant frequency of a harmonic system is inversely proportional to the square root of its mass. We cannot conclude that these physical principles fully account for the ordering of the optima observed because the inherent biomechanics of the joints (e.g., their ranges of motion, lengths, and stiffnesses) may also influence optimal performance characteristics. Nevertheless, an account based on general biomechanical efficiency suffices for the theoretical development to be offered here; the model we introduce does not require a specific model for the oscillation of each limb segment.

The Optimal Selection models applied to finger waving

We turn next to the development of a quantitative fit of the Optimal Selection model to the limb-segment selection data of Rosenbaum et al. (1991). Recall that in the limb-segment selection task subjects oscillated the fingertip over various amplitudes and at various frequencies, using whatever combination of forearm, hand, and finger movement they pleased. The main idea of the Optimal Selection model is that each limb segment (or its corresponding representation) independently bids on the required movement as if it alone were going to accomplish the oscillation. The strength of each segment's bid is assumed to be based on the similarity between the required amplitude and the segment's optimal amplitude, and on the similarity between the required frequency and the segment's optimal frequency. The bids of the three segments are combined to determine the movement of the fingertip.[1]

For purposes of fitting the Optimal Selection model to the data of Rosenbaum et al. (1991), two variants of the model can now be considered. They are based on two ways of characterizing the optimal performance of each limb segment when it is used separately. The two models differ with respect to the rule used to evaluate similarity between required performance and the optimal performance of each segment. One version, the Relative Optimum model (Figure 3), emphasizes between-segment differences in optimal performance points within the amplitude-frequency domain (see points P_f, P_h, and P_a in Figure 3). The other version, the Optimal Amplitude model (Figure 4), emphasizes within-segment differences along the optimal performance functions that relate amplitude to frequency (see lines O_f, O_h, and O_a in Figure 4). These two models are now considered in turn.

The Relative Optimum model

The Relative Optimum model begins with the assumption that there is a single frequency and amplitude of optimal performance for each segment. In the case of the single-segment waving task of Rosenbaum et al. (1991), when each of the three segments was individually oscillated an optimal performance point could be deduced. Rosenbaum et al. (1991) observed that when the frequency of movement was specified, the preferred angular displacement produced by each joint was linearly related to frequency; similarly, when amplitude was specified, the preferred frequency produced was linearly related to amplitude. The point of intersection of these two functions represents a unique amplitude-frequency pair (an attractor) that is globally optimal because it is simultaneously the preferred amplitude at that frequency and the preferred frequency at that amplitude. In the model, a comparison is made between the amplitude and the frequency required by the task (point T in Figure 3) with each segment's point of optimal performance (points P_f, P_h, and P_a in Figure 3). Because frequency and amplitude are incommensurable, the abscissa and ordinate scales are expressed as proportions of the maximum frequency, $Max\,F$, and maximum amplitude, $Max\,A$, respectively. For each segment, i, the distance between the task point and the

[1] When the movement is actually accomplished, all three segments of the arm are assumed to oscillate at the same frequency. While we cannot treat the multisegment arm as a simple oscillator (with a unique stiffness and center of mass), it has been observed that when several joints contribute to movement, the behavior of the arm as a whole can be characterized as that of a passive, multijoint spring (Mussa-Ivaldi, Hogan, and Bizzi, 1985; Hogan, 1985)

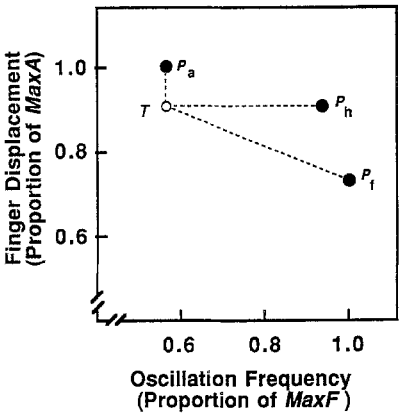

Fig. 3 The Relative Optimum model: Relation of task-required finger displacement and frequency (point T) to optimal performance points of the finger, hand, and arm (points P_f, P_h, and P_a, respectively, as observed by Rosenbaum et al., 1991). (Displacement expressed as a proportion of the maximum optimal amplitude of any segment, $MaxA$, and frequency expressed as a proportion of the maximum optimal frequency of any segment, $Max F$. Dashed lines indicate distances between the task point and the three optimal points.

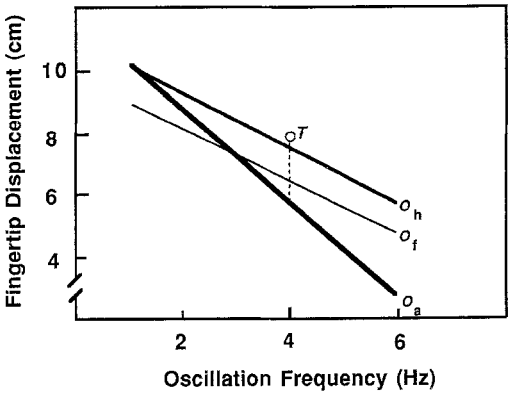

Fig. 4 The Optimal Amplitude model: Optimal performance functions for the finger, hand, and arm that were observed by Rosenbaum et al. (1991), replotted so that the abscissa represents linear displacement of the fingertip. (Lines O_f, O_h, and O_a represent the frequency-driven amplitude performance functions for each segment. Point T represents a hypothetical task point corresponding to a required oscillation of 4 Hz and a required amplitude of 8 cm.)

segment's optimum point can be computed from the weighted sum of the deviations in the amplitude and frequency domains, by the Pythagorean distance formula:

$$d_i = \sqrt{q \cdot \left(\frac{\mathrm{a}(T) - \mathrm{a}(P_i)}{Max\,A}\right)^2 + (1-q) \cdot \left(\frac{\mathrm{f}(T) - \mathrm{f}(P_i)}{Max\,F}\right)^2}. \quad (1)$$

where $\mathrm{a}(P_i)$ and $\mathrm{f}(P_i)$ are the optimal amplitudes and frequencies for the ith segment, respectively, $Max\,A$ and $Max\,F$ are the maximum amplitude and frequency produced by any segment (in this case $Max\,A$ is produced by the arm and $Max\,F$ is produced by the finger), and q is a weighting factor ($0 \leqslant q \leqslant 1$) representing the relative weight given to amplitude differences as against frequency differences. Given the distance, d_i, of the task point from the optimum for each segment, the bid, B_i, for segment i is 1.0 if the required amplitude and frequency coincide with the segment's optimum ($d_i = 0$); otherwise, the bid decreases as d_i increases,

$$B_i = 1 - (t_i \cdot d_i) \quad (0 \leqslant B_i \leqslant 1), \quad (2)$$

where the parameter t_i represents a tuning constant for the ith segment (i.e., the rate at which that segment's bid drops off with the deviation between the required and the optimal task points). A separate tuning constant, t_f, t_h, or t_a, is used to weight the finger, hand, and arm deviations, respectively. The tuning constant represents each segment's sensitivity to differences between the optimum and required task parameters. The proportional contribution, C_i, of the ith segment can be expressed as the ratio of the bid for that segment to the sum of the bids of all s segments:

$$C_i = \frac{B_i}{\sum_{i=1}^{s} B_i}. \quad (3)$$

The Relative Optimum model can be applied to the data of Rosenbaum et al. (1991) by the iterative estimation of the four free parameters (q and the three tuning constants) to minimize the difference between data and model. The model accounts for 78.3% of the variance, $F(1, 22) = 19.85$, $p < .001$ (see Table 1A, top row, and Figure 5, left panel). The model makes the correct qualitative prediction that the majority of movement was produced by the finger, hand, or arm when the required amplitude and frequency matched that segment's optimal amplitude and frequency (main diagonal cells of left panel, Figure 5).

The Optimal Amplitude model

Whereas the Relative Optimum model assumes that each segment has a single point of optimal performance, the Optimal Amplitude model assumes that each segment has an optimal performance function. This function is defined as the set of amplitudes associated with the set of resonant frequencies that can be achieved by change of the segment's stiffness. The optimal performance function for each segment can be estimated by having the subject oscillate with that segment alone at each of several frequencies (see lines O_f, O_h, and O_a in Figure 4). When an optimal performance function exists for a limb segment, it is possible to compute each segment's bid from the difference between a task point, corresponding to a given required

Table 1 Goodness of fit and parameter values for the Relative Optimum and Optimal Amplitude models applied to the finger-waving data, one-bumper tapping data, and two-bumper tapping data

A. The Relative Optimum Model

Task	Percentage of Variance Accounted For	Model Parameters			
		q	t_f	t_h	t_a
Finger Waving	78.3	0.90	5.23	2.82	1.66
One-Bumper Tapping	67.0	0.18	0.38	0.28[a]	1.38[a]
Two-Bumper Tapping	60.9	0.22	0.15	0.26[a]	1.11[a]

B. The Optimal Amplitude Model

Task	Percentage of Variance Accounted For	Model Parameters		
		t_f	t_h	t_a
Finger Waving	44.8	3.33	0.63	0.00
One-Bumper Tapping	63.0	0.08	0.11	0.77
Two-Bumper Tapping	66.9	0.07	0.15	0.90

Note: Parameter q is the amplitude/frequency weighting factor of the Relative Optimum model. The parameters t_f, t_h, and t_a represent the tuning constants for the finger, hand, and arm, respectively, in both models. The finger-waving data come from Rosenbaum et al. (1991). The one-bumper tapping data and two-bumper tapping data come from the present Experiments 1 and 2, respectively.

[a] Parameter for which an increase or decrease of 10% reduced the variance explained by 10% or more

amplitude and frequency, and the optimal performance function. Suppose the bid, B_i, for segment i is 1 if the task point falls on the segment's optimal performance function, but less than 1, down to a minimum of 0, the more the task point deviates from the line. The amplitude or the frequency difference (or some combination of both) can be used to estimate the segment's bid for the required combination of amplitude and frequency. In the waving task of Rosenbaum et al. (1991), the oscillation of all segments had to match the required frequency. Thus, the relevant distance between the required task point and each segment's optimal performance function is the distance between the task amplitude and the optimum function at that frequency:

$$d_i = \left| \frac{\mathrm{a}(T) - \mathrm{a}(O_i, \mathrm{f}(T))}{\mathrm{a}(O_i, \mathrm{f}(T))} \right|. \tag{4}$$

Here, $\mathrm{a}(T)$ denotes the amplitude required by the task, and $\mathrm{a}(O_i, \mathrm{f}(T))$ denotes, for segment i, the optimal amplitude at the task frequency, $\mathrm{f}(T)$. The bid, B_i, and the proportional contribution, C_i, of each segment can be calculated as in Equations 2 and 3, in the same manner as in the Relative Optimum model.

To fit the Optimal Amplitude model, the three tuning constants were adjusted to minimize the variance between the model and the limb-segment selection data of Rosenbaum et al. (1991). The optimal performance functions of the three limb segments were taken directly from the observations of Rosenbaum et al. (1991). The model accounted for 44.8% of the variance in the selection data (see Table 1B, top row, and Figure 5, right panel). The fit of the Optimal Amplitude model was significantly better than would be expected by

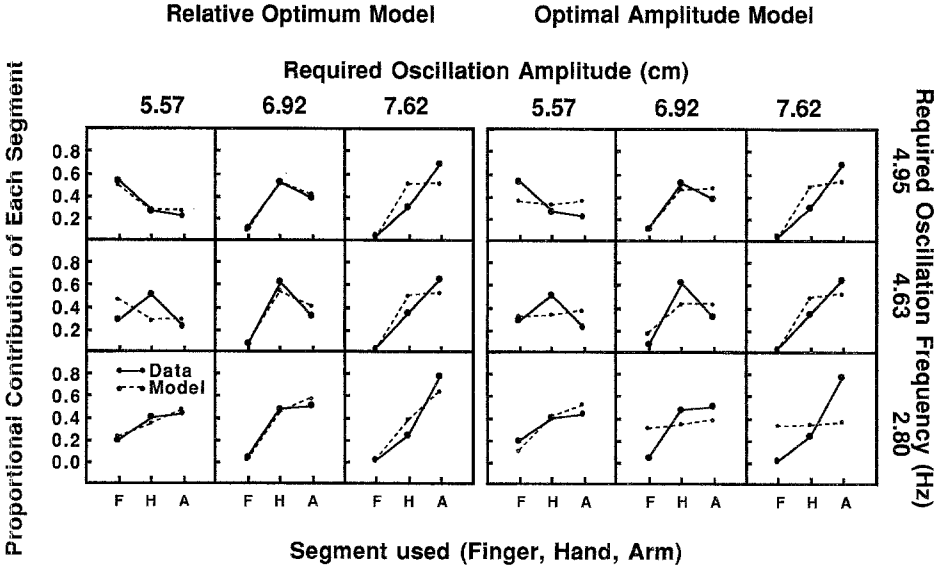

Fig. 5 Selection of movement by the finger, hand, and arm for each of the experimental conditions of the waving task (Experiment 2) of Rosenbaum et al., 1991. (Both panels, solid lines: proportional contribution to displacement of the fingertip in the waving task attributable to movement of the finger (F), hand (H), or arm (A), at each combination of the oscillation amplitudes and frequencies that had been observed to be optimal for the finger, hand, and arm alone in Experiment 1 of Rosenbaum et al., 1991. Left panel, dashed lines: Fit of the Relative Optimum model. Right panel, dashed lines: fit of the Optimal Amplitude model.)

chance alone, $F(1, 22) = 6.22$, $p < .01$. However, the fit was significantly worse than the fit of the Relative Optimum model, $F(1, 22) = 33.96$, $p < .001$, as evaluated by a partial F test that took into account the fact that the Relative Optimum model has one more free parameter than the Optimal Amplitude model (Myers & Well, 1991).

The tuning parameters that produced the best fits for the two models, shown in the first rows of Tables 1A and 1B, varied in a similar manner in both models. The tuning factor was largest for the finger in both models (t_f), and smallest for the arm (t_a). Recall that the tuning factor weights the difference between the required and optimal performances, and so we may interpret this pattern of values to mean that the contribution of the finger is relatively sensitive, and the contribution of the arm relatively insensitive, to changes in the task.

The Optimal Selection models applied to impact control

In the experiment of Rosenbaum et al. (1991), the fingertip's oscillation was unimpeded by any obstacle. We now turn to two new experiments that used a variation of the finger-waving task – repeatedly tapping the finger against one bumper (Experiment 1) and repeatedly tapping the finger back and forth between two bumpers (Experiment 2). We selected these tapping tasks for several reasons. First, tapping, like unobstructed waving, can be achieved with many segment combinations. Second, the task is easily explained to subjects and can be performed easily and reliably without extensive experimental practice. Third, finger-tapping has been used extensively in the motor-control literature, as was mentioned above. Fourth, and most important, the control of impact represents an interesting and challenging extension to the Optimal Selection models. Given that the models, as outlined above, assume optimal performance to be closely related to amplitude and frequency, it is not immediately obvious how the models can be used to explain the control of impacts. The challenge is to extend the models so that they can do so.

Tapping can be viewed as interrupted oscillation. The literal kinematic description of tapping is that the fingertip is displaced in space until it contacts an obstacle, then it comes to rest, and then it is displaced in the opposite direction. An alternative, conceptual, description is that the finger is displaced as if it were moving in a periodic oscillation, where the oscillation is interrupted by collision with an obstacle. We refer to the amplitude that would hypothetically be covered if no obstacle were present as the *virtual amplitude*, and we refer to the location to which the finger would travel at the extreme of its oscillation if no obstacle were present as the *virtual target*. Finally, we refer to the imagined, undisturbed oscillation of the finger through the obstacle as the *virtual oscillation*. In all, the claim that tapping is controlled by deliberately moving over a virtual amplitude to a virtual target can be called the *virtual oscillation hypothesis*.

Virtual oscillation simplifies computation because it allows us to exploit an existing mechanism for the planning and executing of movements. In this respect, the virtual-oscillation hypothesis resembles a model recently proposed for the maintenance of pressure by the hand or other end-effector on a surface (Bizzi, Hogan, Mussa-Ivaldi, & Giszter, 1992). Bizzi et al. proposed that pushing the hand against a surface with a particular force is accomplished by the muscles of the hand and arm being set so that a different posture would be adopted in the absence of the impediment that the surface provides. Because the equilibrium end-point of the adopted posture is "inside" the surface, the spring qualities of the arm exert a constant force against the point of contact. The resulting force depends on the distance between the surface and the hypothetical equilibrium position (the virtual position) of the unconstrained hand.

The virtual-oscillation hypothesis similarly proposes that the displacement of the fingertip during finger tapping can be described as a periodic oscillation, one hypothetical end-point of which is "inside" the obstacle. If the underlying oscillation is sinusoidal (just one of many possibilities) the oscillation observed will be a sinusoid with clipped peaks or troughs.[2] The energy transferred to the obstacle (formally, the impulse of collision) will be determined by the masses of the segments that collide with it and their velocities at the instant of collision. Thus, a subject can generate the same impulse of collision with the finger at high velocity or with the arm at low velocity, since their respective masses differ. The duration of contact with the obstacle should vary with the impulse of collision generated by whichever segments are used.

Figure 6 illustrates these points with two hypothetical oscillations at 2 Hz. The solid line represents the hypothetical trajectory of a large mass, such as the arm, being used to effect a hard impulse of collision, or a smaller mass, such as the hand, being used to effect a soft impulse of collision. The dashed line represents the hypothetical trajectory of a large mass effecting a softer impulse of collision. Thus, the impulse of collision can be altered either by the use of a limb segment of different mass or by a change in the virtual

[2] The motion observed might not take exactly a sinusoidal form, because, apart from noise, the finger might rebound from the obstacle when elastic energy, stored upon colliding with the obstacle, is later released in the form of kinetic energy. The release of elastic strain energy during the recoil helps to optimize efficiency in running and hopping (Alexander, 1984), and so it would also be expected to do so in manual analogues of these behaviors that also require repeated collisions

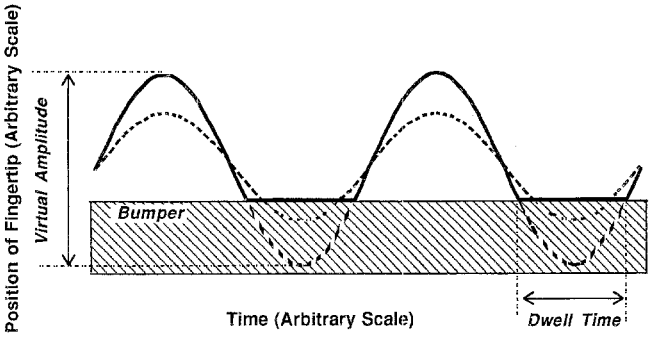

Fig. 6 The virtual-amplitude interpretation of tapping performance. (Dashed line: soft impulse of collision with a segment of large mass. Solid line: hard impulse of collision with a segment of large mass, or soft impulse of collision with a segment of small mass.)

amplitude of the same limb segment in order to modulate velocity at contact. Either version of the Optimal Selection model can be used to predict a particular method of tapping, if these options are borne in mind. Required impacts can be translated into required virtual amplitudes for each segment. The bidding procedure can then be used as before to predict each segment's relative contribution to the movement.

Experiment 1

The one-bumper tapping task

The first experiment was designed to test the virtual-oscillation hypothesis, and to evaluate it with use of the Relative Optimum and Optimal Amplitude models. Subjects were instructed to tap at a required frequency and with a required impulse of collision against a bumper. Three frequencies and three impulses of collision were tested. The main question was what limb segment combination would be used, depending on the frequency and impulse of collision that were required. We expected there to be a switch to more massive segments as the required impulse of collision increased and as the required frequency decreased.

Method

Subjects. Four right-handed university students (one male and three female) between the ages of 20 and 25 participated. Each subject gave written consent and received payment or course credit for participation. The data were collected at the University of Massachusetts, Amherst.

Apparatus and procedure. A WATSMART System (Northern Digital, Inc.) was used to track the movement of four infrared emitting diode markers (IREDs) attached (1) to the side of the distal segment of the subject's right index finger, (2) above the first metacarpal (knuckle) joint, (3) above the wrist, and (4) on the forearm, 15 cm from the wrist marker. The marker positions are shown in Figure 1. The WATSMART System was used to measure the three-dimensional position of each IRED marker to a resolution of 0.1 mm at a sampling rate of 200 Hz.

The impulse of collision was measured by having the fingertip strike a rectangular (15 × 36 mm) bumper, covered with hard rubber (4 mm thick) and attached to a Grass model FT10D force displacement transducer. The displacement rate of the bumper was 0.5 kg/mm, up to a maximum displacement of 1 mm. A Terak computer (LSI-11) monitored the impact of each collision by integrating the force on the force transducer during the 100 ms following contact.[3]

Subjects were asked to produce "soft," "medium," and "hard" collisions. For the experimenters (but not for the subjects), a soft impulse of collision was defined as 0.017 to 0.034 kg · m/s (midpoint 0.026 kg · m/s), a medium impulse of collision was defined as 0.042 to 0.084 kg · m/s (midpoint 0.063 kg · m/s), and a hard impulse of collision as 0.108 to 0.216 kg · m/s (midpoint 0.162 kg · m/s). Subjects received feedback about each impulse of collision from an array of eight light-emitting diodes (LEDs). The diode array was controlled by the Terak computer and was placed in front of the subject so that he or she could easily see it. During the tapping phase of the trial, feedback was provided immediately after each tap. If the impulse of collision was too small, two LEDs lit up; if the impulse of collision was too large, eight LEDs lit up; and if the impulse of collision was within the required range, six LEDs lit up. Subjects were instructed to tap so that six LEDs would light with every tap.

During testing, the subject sat on a stool, 48 cm high, next to a table, 47 cm high, to which the apparatus was attached. The bumper was 17 cm above the table surface and was oriented vertically, with its striking surface parallel to the subject's midsagittal plane. All parts of the apparatus were either painted black or covered in black material to minimize IRED reflection, as is required for accurate use of the WATSMART.

To convey required tapping frequencies to the subject, a series of computer-generated tones was produced on a Macintosh Plus computer. At the beginning of each trial, a low-frequency tone (300 Hz) sounded for 2.5 s, during which time subjects were supposed to hold the index finger motionless against the bumper. The low-tone period was included to provide a baseline for each trial. Next, a series of beeps (100 ms, 900 Hz) sounded at a rate of 1, 3, or 5 beeps per second for 10 s, during which time subjects were supposed to tap with the beeps, striking the bumper when each beep sounded. The frequencies to be tested (1, 3, and 5 Hz) were selected to encompass and extend the range of frequencies of oscillation that subjects spontaneously produced in Rosenbaum et al. (1991). Subjects moved the fingertip horizontally, attempting to strike the middle of the bumper with the intersection of the two most distal segments of the index finger. They could move the fingertip toward and away from the bumper by flexing and extending the index finger, by flexing and extending the wrist, or by adducting and abducting the elbow. The upper arm was not fixed. Subjects were allowed to use their limb segments freely and were instructed to move "as naturally as possible." After 10 s of tapping, the computer sounded a second low

[3] The measurement of impulse of collision was independently calibrated by mounting the force transducer's bumper at one end of a linear air track. Two air-track vehicles (with masses of 146.8 g and 283 g, respectively, and equipped with spring bumpers) were each manually launched down the air track for 25 collisions with the bumper at a variety of speeds. A photocell gate determined the vehicle's velocity just before collision. The recorded impulse of collision was linearly related to the impulse computed from the mass and velocity of the vehicle for impulses up to 0.250 kg · m/s ($r^2 = .97$)

tone (300 Hz) for 2.5 s, during which time subjects were again supposed to hold the index finger motionless against the bumper, for calibration purposes.

Each subject tapped the bumper at each of the nine frequency-impulse combinations of impulse conditions (soft, medium, and hard) and frequency conditions (slow, medium, and fast), in a different random order. Before each data-collection period, the subject was told what condition would be tested (e.g., "soft impact, slow rate"), and allowed to practice the forthcoming combination of frequency and impulse, relying on the LEDs for feedback. The entire session lasted about 1 hour.

Data analysis. The marker positions at the point of contact and at the maximum amplitude of the backswing were used to calculate the proportion of movement of the fingertip attributable to rotation of the finger about the knuckle, to rotation of the hand about the wrist, and to displacement of the forearm along the axis of fingertip movement. The calculations were based entirely on geometry, and did not involve estimates of kinetic (torque-related) influences. Knuckle flexion was estimated by measurement of the change in the angle of intersection of the fingertip-knuckle segment and the knuckle-wrist segment, between the maximum backswing and bumper contact (see Figure 1). The finger's contribution to the displacement of the fingertip was calculated from the change in the angle of knuckle flexion and the distance between the fingertip marker and the knuckle marker. Wrist flexion was estimated from the change in the angle of intersection between the knuckle-wrist segment and the wrist-forearm segment, again between the maximum backswing and bumper contact. The hand's contribution to the displacement of the fingertip was calculated from the wrist flexion and the distance between the fingertip and the wrist joint. Finally, arm contribution to fingertip displacement was determined from displacement of the more distal mark on the forearm. Because the arm-marker movement was parallel to the fingertip movement, it indicated the contribution of the arm to fingertip displacement, whether the movement resulted entirely from elbow or shoulder adduction, or from a combination of the two.

The data were analyzed with a repeated-measures analysis of variance(ANOVA) based on a 3 (Impulse of collision: 0.026, 0.063, or 0.162 kg·m/s) × 3 (Frequency of tapping: 1, 3, or 5 Hz) design. Each trial's means were based on 8 to 48 collisions in 10 s, depending on the tapping frequency. The first and last collisions in a sequence were not used because of potential variation in the beginnings and ends of the sequence, and collisions early in a trial were excluded if the amplitudes appeared markedly different from later, stable performance.

Results

Modulation of impulse of collision. The first analysis was designed to check that subjects successfully varied the impulse of collision in the Soft, Medium, and Hard conditions. Because neither the voltages from the force transducer nor the onsets or offsets of the lights were permanently recorded, the check was made by estimation of the velocity of the fingertip when it struck the bumper. Velocity at contact was estimated by measurement of the displacement of the fingertip in the two timesteps (10 ms) that preceded first contact with the bumper.

As is shown in Table 2, velocity at impact depended on the required impulse of collision, $F(2, 6) = 7.11$, $p = .026$. As was expected, impact velocity increased with required impulse of collision. Required frequency had no significant effect on impact velocity, $F(2, 6) = .57$, and there was no required Impulse by Frequency interaction, $F(4, 12) = .214$.

Table 2 Fingertip Velocity (m/s) at impact with the bumper in Experiment 1, by tapping frequency and impulse of collision

Tapping Frequency (Taps/s)	Required Impulse of Collision (kg·m/s)		
	0.026	0.063	0.162
1	1.25 (0.21)	1.33 (0.10)	1.68 (0.14)
3	1.42 (0.15)	1.58 (0.25)	1.88 (0.35)
5	1.21 (0.16)	1.50 (0.13)	1.82 (0.17)

Note: Averaged across the recorded taps of 4 subjects. Standard errors are in parentheses

Modulation of virtual amplitude: Amplitude of the backswing. The virtual-oscillation hypothesis predicted that subjects would modulate the impulse of collision by varying the virtual amplitude. It also predicted that as tapping frequency increased, virtual amplitude would decrease, because as frequency increases, a smaller virtual amplitude suffices to produce the same velocity at impact.

To test these predictions, we needed to estimate virtual amplitudes. We reasoned that virtual amplitudes could be estimated by measurement of the observed amplitudes of backswings. That is, assuming a symmetric or roughly symmetric oscillation, the location to which the finger travels when opposite the barrier should reveal how far the finger would have travelled through the barrier in its absence.

As is shown in the leftmost panel of Figure 7, the amplitude of the backswing increased with required impulse of collision, $F(2, 6) = 12.05$, $p = .008$, and decreased with required frequency, $F(2, 6) = 6.45$, $p = .032$. Both results confirm the predictions. The interaction of Impulse and Frequency was also significant, $F(4, 12) = 3.26$, $p = .05$.

Selection of finger, hand, and arm movements. To determine the relative contributions of the finger, hand, and arm to the displacement of the fingertip, the relative contributions observed were estimated from the kinematic data.

The proportional contributions of the finger, hand, and arm are shown as solid lines in each panel of Figure 8. As in the finger-waving study of Rosenbaum et al. (1991), the proportional contribution of the finger, hand, and arm varied with the experimental condition. The proportional contribution of the finger decreased with the required impulse of collision, $F(2, 6) = 10.54$, $p < .02$, but there was no impulse effect for the proportional contribution of the wrist, $F(2, 6) = 0.60$, and only a marginally significant effect for the arm, $F(2, 6) = 3.56$, $p < .10$. No frequency effect was found for the proportional contribution of the

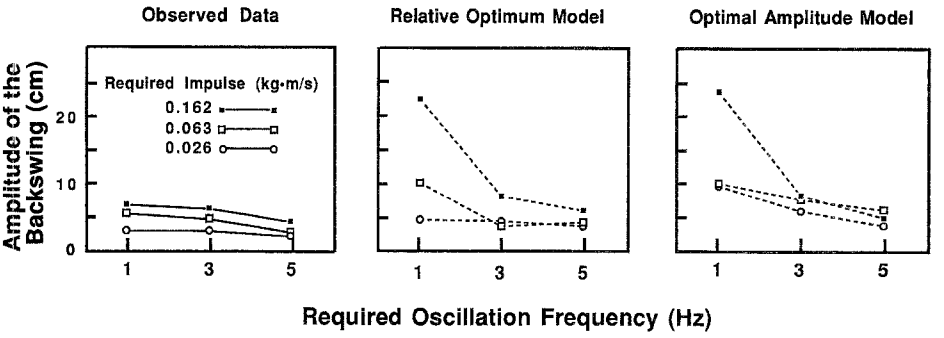

Fig. 7 Amplitude of the backswing (greatest distance between the fingertip and the surface of the bumper) for the experimental conditions of the one-bumper tapping experiment (Experiment 1). (Left panel: observed data; center panel: predictions of the Relative Optimum model; right panel: predictions of the Optimal Amplitude model.)

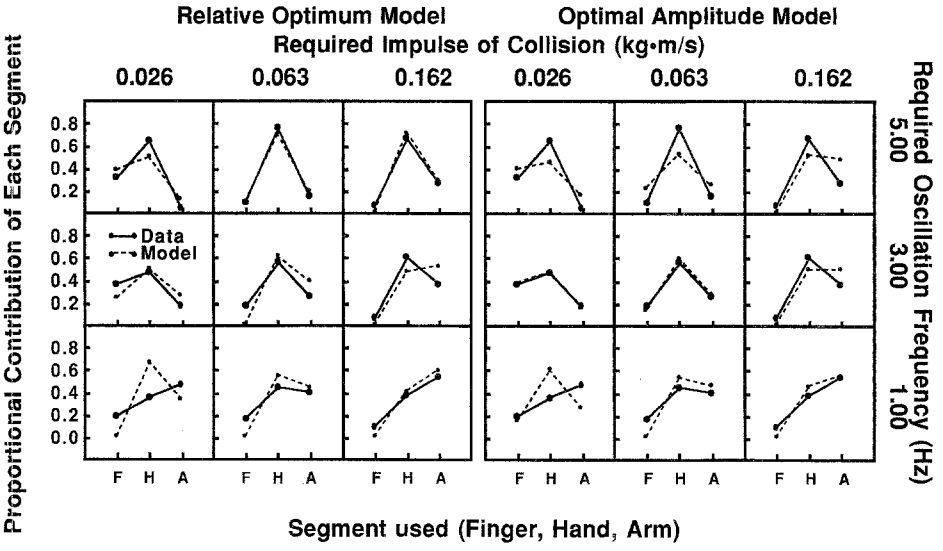

Fig. 8 Selection of movement by the finger, hand, and arm for each of the experimental conditions in the one-bumper tapping experiment (Experiment 1 of the present study). (Both panels, solid lines: proportional contribution to displacement of the fingertip attributable to movement of the finger (F), hand (H), or arm (A); left panel, dashed lines: Fit of the Relative Optimum model. Right panel, dashed lines: fit of the Optimal Amplitude model.)

finger, $F(2, 6) = 0.40$, but the proportional contribution of the wrist increased with the required frequency, $F(2, 6) = 24.62$, $p < .01$, and the proportional contribution of the arm decreased with the required frequency, $F(2, 6) = 13.67$, $p < .01$. There were no significant Impulse by Frequency interactions for the finger, hand, or arm.

Application of the Optimal Selection models

To fit the Optimal Selection models to the tapping data, we determined, for each required task frequency, f(T), the virtual amplitude, A_i, that would be required for the ith limb segment alone to produce the required impulse of collision, I, based on that segment's estimated effective mass, m_i. In these computations the required impulse of collision was given by the definition of the task. The masses of the finger, hand, and arm were estimated by water displacement, with the use of the corresponding segment(s) of the first author's right arm; the values measured were 32,605, and 1800 g, respectively; the effective mass, m_i, used in the computations was corrected for the distance from the center of mass of each segment to the fingertip and to the segment's center of rotation. Next, each segment's bid for each task was computed from the amplitude it would be required to oscillate if it alone generated the required impulse of collision through a collision with the bumper, with the other joints assumed to be rigid. On the assumption that the fingertip was in contact with the bumper during 32% of each oscillation cycle (the average value observed across conditions), the impulse of collision produced by segment i acting alone is twice the product of the effective mass and the velocity of the segment when it collides with the bumper; the velocity depends, in turn, on the frequency of the virtual oscillation, its amplitude, and the phase of oscillation at the beginning of contact with the bumper (a phase of 0.18 π radians at collision corresponds to contact during 32% of the cycle), so that

$$I = 2 \cdot m_i \cdot f \cdot A_i \cdot \cos(0.18\pi). \quad (5)$$

The virtual amplitude required for segment i to produce the required impulse of collision is, therefore,

$$A_i = \frac{I}{2 \cdot m_i \cdot f \cdot \cos(0.18\pi)}. \quad (6)$$

The next step in the model evaluation is to determine how well the performance of the subjects in Experiment 1 can be predicted on the basis of the optimum performance characteristics of the subjects of Rosenbaum et al., 1991.

Fit of the Relative Optimum model. Each segment's bid was based on the proximity of the computed virtual amplitude to that segment's optimal amplitude and frequency. The bid was computed by substitution of the virtual amplitude, A_i, for the required task amplitude, $a(T)$, in Equation 1. The proportional contribution of each segment, C_i, was based on its bid relative to all the bids, as prescribed by Equations 2 and 3. When the tuning parameters were adjusted for the best fit to the data, 67.0% of the variance in movement selection was accounted for, $F(1, 22) = 11.167, p < .005$ (Table 1A, middle row). The best-fitting values are shown along with the obtained values in the left panel of Figure 8, where it is seen that the model performed in a qualitatively accurate way, supporting the extension of the Relative Optimum to impact control.

The Relative Optimum model was also used to predict the amplitude of the backswing of the tap (maximum distance of the fingertip from the surface of the bumper). This estimate was obtained directly from the model with no additional free parameters, by the simple summing of the previously calculated virtual amplitudes of each segment, weighted by its proportional contribution to finger displacement, and on the assumption of a contact duration of 32%, as above. The correlation between estimated and observed amplitude of the backswing was significant, $r = .77$, $t(7) = 3.193$, $p < .01$. However, comparison of the model's estimates (center panel of Figure 7) with the observed data (left panel of Figure 7) showed that despite the significant correlation, the model tended to overestimate the amplitude of the backswing.

Fit of the Optimal Amplitude model. Each segment's bid was based on the proximity of the computed virtual amplitude to that segment's optimal performance function at the required frequency, by substitution of the virtual amplitude, A_i, for the required task amplitude, $a(T)$, in Equation 4. The proportional contribution of each segment, C_i, was based on its bid relative to all the bids, as in Equations 2 and 3. When the tuning parameters were adjusted for the best fit to the data, 63.0% of the variance in movement selection was accounted for, $F(1, 22) = 13.054, p < .005$ (Table 1B, middle row). The best-fitting values are shown, along with the observed values, in the right-hand panel of Figure 8.

The Optimal Amplitude model's prediction of the amplitude of the backswing was calculated in the same manner as described for the Relative Optimum model. These estimates (right panel of Figure 7) also correlated highly with the observed data, $r = .71$, $t(7) = 2.668$, $p < .025$. The Optimal Amplitude model also tended to overestimate the amplitude of the backswing, though not so much as the Relative Optimum model.

Summary of results. The contribution of the three segments of the forearm to finger displacement varied systematically, consistently with the virtual-amplitude hypothesis. The two Optimal Selection models were able to account for a large proportion of the variation in segment contribution, and both models captured the qualitative characteristics of the variation in the observable portion of movement amplitude. Both models performed about equally well.

Experiment 2

The two-bumper tapping task

In Experiment 2, the subject's task was to strike two bumpers with the fingertip at prescribed frequencies (2, 4 or 6 taps per second, corresponding to oscillation frequencies of 1, 2, and 3 Hz) and with prescribed impulses of collision (0.026, 0.063, or 0.162 kg · m/s).[4] The separation between the bumpers ranged from 3.8 to 11.4 cm. In contrast to the tapping task in Experiment 1, in which the movement of the fingertip was constrained at only one extreme of displacement, in the two-bumper task movement of the fingertip was constr ained at both endpoints of oscillation. We expected the Optimal Selection models to apply to two-bumper tapping as well, however. As before, we predicted that required impulses could be converted to virtual amplitudes, and from the virtual amplitudes (along with the required frequencies) it would be possible to assign bids to the effectors, which in turn could give rise to empirically realistic relative contributions. The main prediction was that there would be a switch to more massive segments as the required impulse of collision increased,

[4] Experiment 2 was actually conducted before Experiment 1, before the WATSMART system was available. It is presented second here because Experiment 1 is more comparable to the earlier published study of Rosenbaum et al. (1991). Because the videotape recording system used in Experiment 2 can only make 30 samples per second, rather than the 200 samples per second provided by the WATSMART system in Experiment 1, the maximum frequency of tapping imposed was 3 Hz, so there would be at least 5 video frames per tap

as the distance between the bumpers increased, and as the required frequency decreased.

A second aim of Experiment 2 was to explore a new measure for testing the virtual-oscillation hypothesis. As applied to tapping on two bumpers, the virtual-oscillation hypothesis assumes that the impulse of collision can be controlled by variation of the virtual amplitude of the movement through the obstacle. In experiment 1, the virtual-amplitude hypothesis was tested by measurement of the backswing of the finger as it moved away from the bumper. In Experiment 2, because there were two bumpers, it was impossible to measure a free backswing. We therefore studied the dwell time of the finger on the bumpers, by measuring the time between the first and last contacts with the bumper in each collision. We predicted that dwell time would increase with virtual amplitude; in other words, when virtual amplitude was expected to increase, dwell time should also increase.

Method

Subjects. Five right-handed subjects each served in a 45-min session. All subjects were students at Hamilton College, where the experiment was conducted.

Apparatus and procedure. High-contrast joint-position markers (0.5-cm black circles of nontoxic make-up on a white surrounding disk) were placed on the fingertip, on the knuckle, on the wrist, and on the forearm 15 cm from the wrist. Performance was videotaped at 30 frames per second, from a point 1 m above a tabletop, with a short exposure duration (1/1000 s) to obtain a clear image of the arm, finger, and hand when individual video frames were frozen in order to digitize the arm, hand, and finger positions. Subjects sat with shoulders parallel to the front edge of the table, with the forearm held horizontally, and with the hand held so that the middle, ring, and little fingers were flexed, the thumb rested on the flexed middle finger, and the index finger pointed out. The hand was oriented so that the most distal joint of the thumb pointed up. The elbow extended slightly beyond the frontal plane of the subject's body, by about 15°.

Two vertically oriented rectangular bumpers (15 × 36 mm) were mounted on Grass model FT10D force transducers and were placed with their centers 15 cm above the tabletop, opposite each other along a horizontal axis rotated 45° counterclockwise with respect to the edge of the table in front of the subject. The surface of each bumper was covered with 4 mm of hard rubber. The more distant bumper was placed directly in front of the subject at 80% of the maximum reach of the subject's fingertip, while the location of the closer bumper was adjusted to produce an interbumper separation of 3.8, 7.6, or 11.4 cm. As in Experiment 1, the strain-gauge output of each transducer was monitored by an LSI-11 computer, which gave the subject visual feedback to indicate if the impulse of collision fell within, above, or below the required range. The required ranges for the soft, medium, and hard impulse collisions were defined as in Experiment 1, and the visual feedback took the same form.

Forty collisions were produced in each trial. At the start of each trial, a Macintosh SE computer generated a series of 40 alternating 440 and 880 Hz tones, each lasting approximately 17 ms, which the subject heard once to prepare for the forthcoming tapping task. When the subject indicated his or her readiness to perform, the tone series was replayed. During the second tone series, subjects were supposed to strike one bumper on each high tone and the other bumper on each low tone.

The experiment had 27 conditions, based on a full crossing of the three required frequencies (2, 4, or 6 taps per second, corresponding to oscillations of 1, 2, or 3 Hz), three required impulses of collision (0.026, 0.063, or 0.162 kg·m/s) and three separations between the bumpers (3.8, 7.6, or 11.4 cm). The conditions were run in a different random order for each subject.

Data analysis

To evaluate the contribution of each segment to the oscillation, it was necessary to measure the joint angles at the two extremes of displacement in each oscillation.[5] To obtain these measures, we used a manual digitizing technique developed by Barnes, Vaughan, Jorgensen, and Rosenbaum (1989). Using a single-frame video editor (Panasonic model AG-1950) and a half-silvered mirror, we optically superimposed the video monitor and a Macintosh II monitor. The mirror was positioned at a 45° angle between the two monitors, which were perpendicular to one another, so that the experimenter could digitize the position of each marker by placing the Macintosh cursor directly over it and clicking the mouse. For each collision, the videotape was positioned on the first frame in which the bumper was struck, and coordinates of the markers on the fingertip, knuckle, wrist, and forearm were digitized. Digitizing was restricted to the 16th–21st collisions, and so three collisions with each bumper were digitized (collisions 16, 18, and 20 for one bumper, and 17, 19, and 21 for the other bumper). The number of frames in which there was fingertip contact with the bumper was also recorded, providing a measure of the duration of contact with the bumper – the *dwell* time (see Figure 6). The positions of the four markers in these three collisions with each bumper were averaged for subsequent analysis.

Results

Contributions of the finger, hand, and arm. The proportional contribution of the finger, hand, and arm to fingertip displacement was first subjected to a repeated-measures ANOVA (3 × 3 × 3 × 3) in which the independent variables were the Separation between the bumpers, the required Frequency of oscillation, the required Impulse of collision, and the Segment used. A number of two- and three-way interactions involving the segment variable were significant, indicating that the independent variables had different effects on the proportional contribution of the segments (as is shown in the leftmost panel of Figure 8); there were no significant main effects or interactions that did not involve the segment variable. Because these interactions indicated that the effects of the independent variables varied from one segment to another, the proportional contribution data were submitted to a separate 3 × 3 × 3 ANOVA for each of the three segments, where the independent variables were the Separation between the bumpers, the required Frequency of alternation, and the required Impulse of collision. In the discussion to follow, we first present each interaction that was significant in the

[5] Recording the joint angles at intermediate displacements would have been desirable from the standpoint of characterizing the kinematics of the entire movement, but was considered unnecessary from the standpoint of characterizing the contributions of the limb segments at the time of collision

omnibus ANOVA. We then present the analyses for individual segments, describing how the proportional contribution of each segment depended on the task requirements.

The required impulse of collision affected the proportional contribution to fingertip displacement of the three limb segments, $F(4, 16) = 19.60, p < .0001$ (see Table 3). Finger contribution declined with required impulse of collision, $F(2, 8) = 35.41, p < .0001$, whereas arm contribution increased with required impulse, $F(2, 8) = 21.43, p < .0006$. Hand contribution was greatest at the intermediate impulse condition, though the effect fell short of significance, $F(2, 8) = 3.89$, $p = .066$.

The separation between the bumpers affected the relative contributions of the three limb segments, $F(4, 16) = 6.82, p < .003$ (see Table 4). Finger contribution declined with separation, $F(2, 8) = 7.88, p < .02$, whereas hand contribution increased, $F(2, 8) = 4.56$, $p < .05$, as did arm contribution, $F(2, 8) = 10.75$, $p < .006$.

Required frequency also affected the relative contributions of the three limb segments, $F(4, 16) = 6.67$, $p < .003$ (see Table 5). Hand contribution increased with required frequency, $F(2, 8) = 5.63, p < .03$, whereas arm contribution decreased, $F(2, 8) = 27.48$, $p < .0003$. Finger contribution was not significantly affected by tapping frequency.

Bumper Separation and required Impulse of collision had interactive effects on the relative contributions of the limb segments, $F(8, 32) = 3.80, p < .01$. The relative contribution of the finger was greatest at the smallest required impulse of collision and shortest bumper separation, $F(4, 16) = 4.75, p < .02$; conversely, the relative contribution of the arm was least under these conditions, $F(4, 16) = 3.33, p < .04$ (see Table 6). The finger made its greatest contribution at small bumper separations and soft impulse magnitudes, but either a hard impulse magnitude or a larger separation resulted in more hand or arm movement.

Required Frequency and bumper Separation also had interactive effects on the contribution of the limb segments, $F(8, 32) = 3.16, p < .01$ (see Table 7). The interaction of Separation and required Impulse of collision was significant for the finger, $F(4, 16) = 3.15$, $p < .05$, and for the hand, $F(4, 16) = 4.22, p < .02$, but not for the arm.

To summarize the results, an increase in either required impulse of collision or bumper separation caused a shift in the proportional contribution from the finger to the hand, and even more to the arm. Thus, finger contribution was greatest at the shortest separation and smallest impulse conditions, whereas arm contribution was greatest at the largest separation and largest impulse conditions. By contrast, an increase in required frequency produced a shift in contribution from the arm to the hand and, to a lesser extent, to the finger.

Table 3 Proportional contribution of finger, hand, and arm segments of fingertip displacement in Experiment 2, by impulse of collision

	Required Impulse of Collision (kg · m/s)		
Segment	0.026	0.063	0.162
Finger	0.27	0.08	0.03
Hand	0.50	0.57	0.49
Arm	0.22	0.34	0.48

Note: Averaged over repetition frequencies and bumper separations. Columns may not sum to 1.00 because of rounding

Table 4 Proportional contribution of finger, hand and arm segments to fingertip displacement in Experiment 2, by bumper separation

	Bumper Separation (cm)		
Segment	3.8	7.6	11.4
Finger	0.26	0.09	0.04
Hand	0.44	0.56	0.57
Arm	0.30	0.35	0.40

Note: Averaged over repetition frequencies and impulse magnitudes. Columns may not sum to 1.00 because of rounding

Table 5 Proportional contribution of finger, hand and arm segments to fingertip displacement in Experiment 2, by tapping frequency

	Tapping Frequency (Taps/s)		
Segment	2	4	6
Finger	0.11	0.13	0.15
Hand	0.44	0.51	0.61
Arm	0.44	0.36	0.24

Note: Averaged over bumper separations and impulse magnitudes. Columns may not sum to exactly 1.00 because of rounding

Modulation of virtual amplitude: Dwell time. In the two-bumper tapping task, oscillation was constrained at both extremes of movement, so we could not look at the amplitude of the backswing (as in Experiment 1) to provide an indication of the virtual amplitude of oscillation. Instead, we examined the duration of contact with the bumper (dwell time), expecting it to be longer in those conditions that theoretically required larger virtual amplitudes. With dwell time as the dependent measure (see Figure 9, left panel), the interaction of Impulse, oscillation Frequency, and bumper Separation was significant, $F(8, 32) = 5.25, p < .0005$. Dwell time was longer at lower frequencies, smaller separations, and larger required impulses of collision.

Table 6 Proportional contribution of finger, hand, and arm segments to fingertip displacement in Experiment 2, by impulse and bumper separation

Required Impulse of Collision (kg·m/s)	Segment	Bumper Separation (cm) 3.8	7.6	11.4
0.026	Finger	0.48	0.22	0.11
	Hand	0.39	0.55	0.58
	Arm	0.13	0.23	0.31
0.063	Finger	0.23	0.03	−0.01[a]
	Hand	0.47	0.63	0.62
	Arm	0.29	0.34	0.39
0.162	Finger	0.07	0.01	0.01
	Hand	0.45	0.51	0.50
	Arm	0.48	0.47	0.49

Note: Averaged across repetition frequencies. Columns in each panel may not sum to 1.00 because of rounding.
[a] The negative value for finger contribution resulted from the finger's bending backwards because of the collision with the bumper

Table 7 Proportional contribution of finger, hand, and arm segments to fingertip displacement in Experiment 2, by tapping frequency and bumper separation

Tapping Frequency Taps/s	Segment	Bumper Separation (cm) 3.8	7.6	11.4
2	Finger	0.30	0.06	−0.04[a]
	Hand	0.31	0.49	0.53
	Arm	0.38	0.44	0.51
4	Finger	0.25	0.06	0.08
	Hand	0.42	0.58	0.53
	Arm	0.32	0.37	0.39
6	Finger	0.23	0.14	0.07
	Hand	0.58	0.62	0.63
	Arm	0.19	0.24	0.29

Note: Averaged across repetition frequencies. Columns in each panel may not add to 1.00 because of rounding.
[a] The negative value for finger cntribution resulted from the finger's bending backwards because of the collision with the bumper

Fit of the Optimal Selection models

The next step was to fit the Optimal Selection models to the data from the two-bumper task. The amplitude for which each segment's bid was calculated was the virtual amplitude of each segment (i.e., the fingertip displacement that the segment would have had to produce to achieve the required impulse of collision by itself). The virtual amplitude necessary to accomplish the required impulse of collision was calculated for each segment in each experimental condition in a manner similar to that used in Experiment 1. First, we noted that the magnitude, I, of the impulse of collision for the ith segment is related to that segment's effective mass, m_i, the virtual amplitude, A_i, and the required task frequency, $f(T)$, as follows:

$$I = 2 \cdot m_i \cdot \mathrm{f}(T) \cdot A_i \cdot \cos\left[\sin^{-1}\frac{d}{A_i}\right]$$

$$= 2 \cdot m_i \cdot \mathrm{f}(T) \cdot A_i \cdot \sqrt{1 - \left[\frac{d}{A_i}\right]^2}, \qquad (7)$$

where d denotes the distance between the bumpers. Note that the virtual amplitude, A_i, must be greater

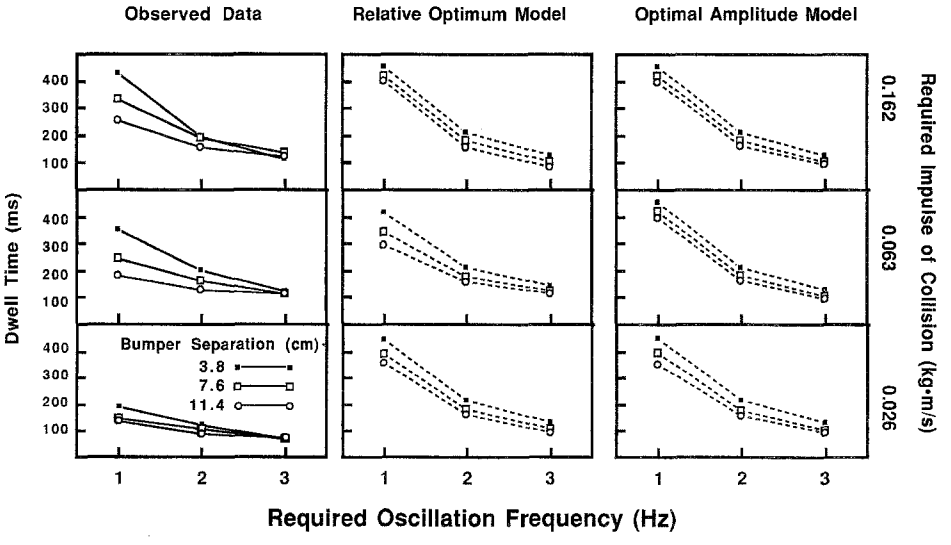

Fig. 9 Dwell time (time in contact with the bumper during each tap) for the experimental conditions of the two-bumper tapping experiment (Experiment 2). (Left panel: observed data; center panel: predictions of the Relative Optimum model; right panel: predictions of the Optimal Amplitude model.)

than the distance between the bumpers or the fingertip will not strike both of them. Solving for A_i gives the required virtual amplitude for the ith segment:

$$A_i = \sqrt{\frac{I^2}{4 \cdot [m_i]^2 \cdot [\mathrm{f}(T)]^2} + d^2}. \quad (8)$$

Equation 8 implies that the calculated virtual amplitudes should be larger for the finger than for the hand, and larger for the hand than for the arm, owing to the differences in the masses of these limb segments. In addition, Equation 8 implies that the virtual amplitudes should decrease with required frequency, $\mathrm{f}(T)$, and increase with bumper separation, d.

Fit of the Relative Optimum model. As in Experiment 1, at each required frequency each segment's bid was computed from the proximity of its virtual amplitude (from Equation 8) to its optimal amplitude and frequency, by substitution of the virtual amplitude, A_i, from Equation 8 for the required task amplitude, $\mathrm{a}(T)$, in Equation 1. The proportional contribution of each segment, C_i, was based on its bid in relation to all the bids, as given by Equations 2 and 3. When the tuning parameters were adjusted for the best fit to the data, 60.9% of the variance in movement selection was accounted for, $F(1, 76) = 29.593$, $p < .001$ (Table 1A, bottom row). The predicted segment contributions are shown along with the observed segment contributions in the left panels of Figures 10a, 10b, and 10c.

The Relative Optimum model was also used to predict the dwell times in each of the 27 conditions of Experiment 2. This prediction required no new free parameters. Instead, dwell times were derived by the summing of the virtual amplitudes, A_i, for each segment, weighted by the contribution, C_i, of each segment to the overall movement. The predicted dwell time was computed from this weighted sum, assuming (for simplicity) a symmetrical sinusoidal virtual trajectory that overlapped each bumper equally. The model generated a pattern of dwell times that was similar to the observed dwell times (cf. Figure 8, left and center panels). The overall correlation between model and observed dwell times was high ($r = .79$) and statistically significant, $t(25) = 6.423$, $p < .001$. However, the model overestimated dwell times at the slowest tapping rate and underestimated it at the fastest tapping rate, as can be seen by comparison of the left and center panels of Figure 8.

Fit of the Optimal Amplitude model. The computed virtual amplitudes were compared to the optimal performance functions of the three limb segments (Equation 4) to calculate the bid, B_i, for each segment, by use of Equation 2. The proportional contribution of each segment, C_i was then determined, by means of Equation 3. The model accounted for 66.9% of the variance, $F(1, 77) = 51.876$, $p < .001$ (Table 1B, bottom row, and right panels of Figures 10a, 10b, and 10c).

The Optimal Amplitude model was also used to predict the dwell times. The model generated a pattern of dwell times similar to the observed dwell times (compare left and right panels of Figure 8). The overall correlation between model and observed dwell times was high ($r = .79$) and statistically significant, $t(25) = 6.423$, $p < .001$, though it does not differ from the correlation observed with the Relative Optimum model. Furthermore, like the Relative Optimum model, the Optimal Amplitude model tended to overestimate dwell times, particularly at the lowest tapping rate.

Summary of results

In Experiment 2, as in Experiment 1, the contributions of the three segments varied in a manner consistent with the virtual-oscillation hypothesis. The two versions of the Optimal Selection model accounted for a large amount of the variation in segment contribution, and both versions captured the qualitative characteristics of the variation in dwell time. That they did so attests to the generality of the hypothesis and to the (apparent) validity of the virtual-amplitude idea. The data are consistent with the hypothesis that subjects aim for points that are past impact surfaces to generate impacts of collision.

As in the case of the application of the models to the finger-waving task of Rosenbaum et al. (1991), the relative values of the tuning parameters that produced the best fit for both models, shown in the second and third rows of Tables 1A and 1B, demonstrated the same relative pattern across segments. However, in contrast to the finger-waving task, in the two tapping tasks the contribution of the finger was relatively insensitive to task variation (as is shown by a relatively small value of t_f), whereas the contribution of the arm was in each case most sensitive to task variation. This observation argues against the interpretation of the tuning constants as directly representing some biomechanical characteristic of each segment. How, then, are we to interpret the difference in the ordinal relations among the three parameters across tasks?

One plausible interpretation takes note of the relative range of performance required by the two kinds of task. In the waving task, the variation of both amplitude and frequency of required fingertip displacement was small in comparison to that required in the tapping tasks, and much of the task was in the domain of performance that could easily be accomplished by the finger alone. By contrast, the range of performance required in the tapping tasks was larger, and the required displacements were often not achievable by the finger alone. As a consequence, in the tapping tasks the allocation of movement to the different segments was most sensitive to the concordance of task requirements with the arm's optimal contribution.

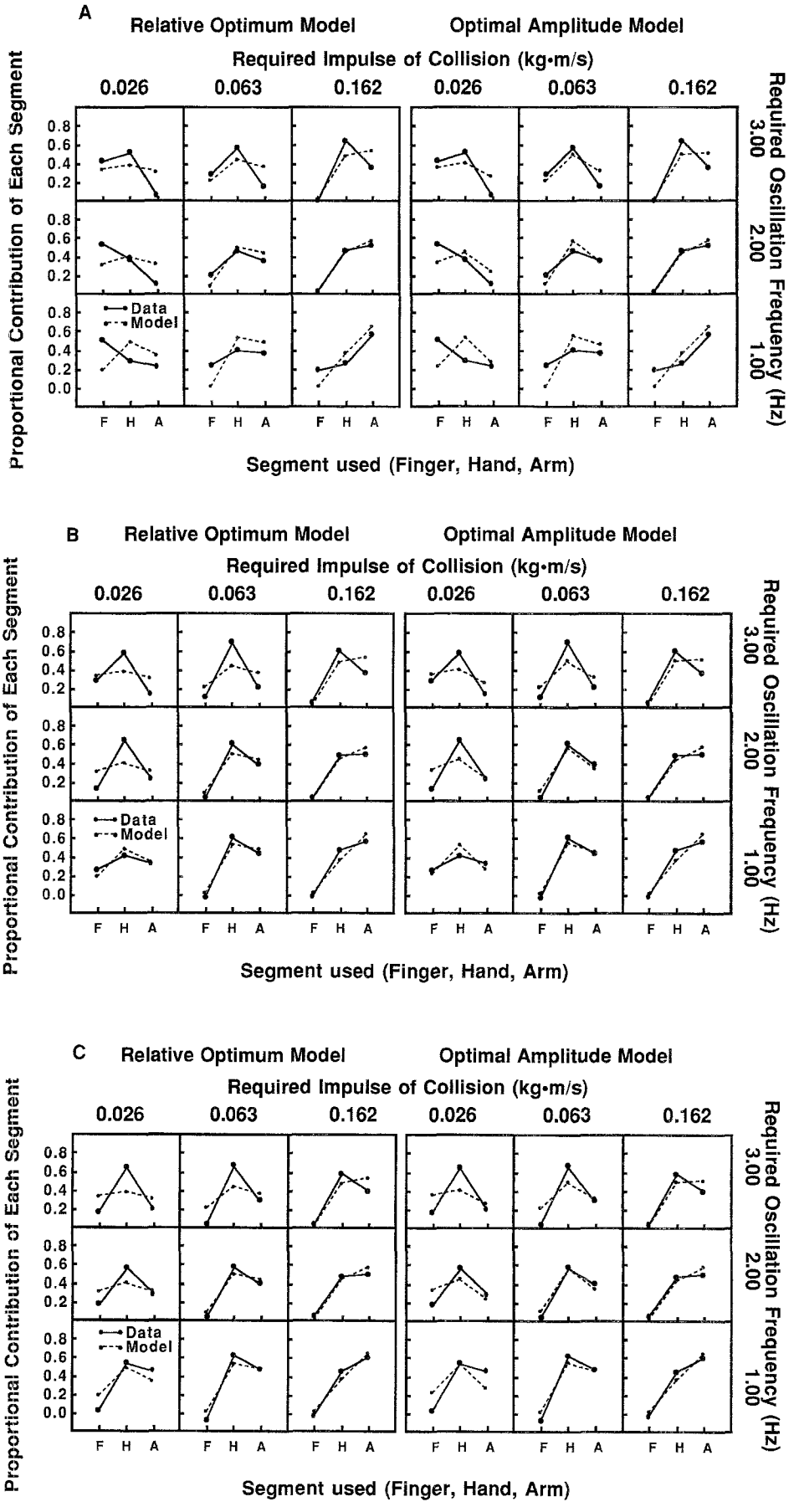

Fig. 10 Selection of movement by the finger, hand, and arm for each of the experimental conditions in the two-bumper tapping experiment. (A. Bumpers separated by 3.8 cm. B. Bumpers separated by 7.6 cm. C. Bumpers separated by 11.4 cm. All graphs, solid lines: proportional contribution to displacement of the fingertip attributable to movement of the finger (F), hand (H), or arm (A); left panel of each graph, dashed lines; fit of the Relative Optimum model; right panel of each graph, dashed lines: fit of the Optimal Amplitude model.)

Sensitivity of models to parameter settings

In addition to goodness of fit and simplicity, another criterion that is important in evaluating the adequacy of a model is its sensitivity to changes in the values of its free parameters. It is desirable for a model's fit not to be highly dependent on its parameter values. The sensitivity of the two models' fit to the data of all three experiments was evaluated by computation of their goodness of fit when each of the model's parameters was individually increased or decreased by 10% of its best-fitting value. Table 1 indicates which of the parameters proved to be sensitive by this criterion. A 10% change in two of the best-fitting parameter values of the Relative Optimum model reduced the variance explained in each of the tapping experiments by 10% or more, whereas none of the parameter values of the Optimal Amplitude model was as sensitive as this. The pattern of sensitivity to parameter change also reflects the fact that the Relative Optimum model fit best when applied to the finger-waving data. The Optimal Amplitude model achieved essentially the same fit as the Relative Optimum model with one free parameter less when applied to the one- and two-bumper tapping tasks, and none of its parameter values was sensitive by the 10% criterion.

Alternative models

We considered a number of other models in the course of analyzing the data from the three experiments discussed here. The simplest alternative model we considered is one in which the bid of each segment is proportional to the virtual amplitude on each trial. This model, with three free parameters (the proportion contributed by each segment), accounted by 42.8, 58.7, and 28.4% of the variance in the finger-waving, one-bumper tapping, and two-bumper tapping experiments, respectively; these values are markedly worse than the values of either of the optimal-selection models.

A second alternative model is one in which the bid of each segment is linearly related to the virtual amplitude. This model, with six free parameters (the slope and intercept of the bid function for each segment), accounted for 82.0% of the variance in the waving task, which is significantly better than the Optimal Amplitude model, $F(1, 20) = 13.78$, $p < .005$, but not significantly better than the Relative Amplitude model, $F(1, 20) = 2.06$, $p > .10$. The six-parameter model also accounted for 80.8% of the variance in the one-bumper tapping task, which is significantly better than the Optimal Amplitude model, $F(1, 20) = 6.18$, $p < .025$, and the Relative Optimum model, $F(1, 20) = 7.19$, $p < .025$; and it accounted for 76.2% of the variance in the two-bumper tapping task, which is significantly better than the Optimal Amplitude model, $F(1, 74) = 9.64$, $p < .005$, and the Relative Optimum model, $F(1, 74) = 23.79$, $p < .001$. However, several features of the alternative model were unsatisfactory. The fit to the waving data was highly sensitive to the particular parameter values that were chosen; the model's predictions (for the waving data) did not change with task frequency; and the pattern of best-fitting parameter values was different across the three tasks.

A final alternative model that we considered is identical to the Relative Optimum model, except that the optimal amplitude and frequency of performance of each segment were estimated as free parameters rather than fixed at the values observed in the experiment of Rosenbaum et al. (1991). The variance accounted for, with 10 free parameters (the 4 parameters q, t_f, t_h, and t_a of the Relative Optimum model, and the two parameters $a(P_i)$ and $f(P_i)$ for each of the three segments), was 92.4% for the waving task, which was significantly better than the Optimal Amplitude model, $F(1, 16) = 14.32$, $p < .005$, and the Relative Optimum model, $F(1, 16) = 4.95$, $p < .05$; 76.2% for the one-bumper tapping task, which was not significantly better than the Optimal Amplitude model, $F(1, 16) = 1.27$, $p > .25$, or the Relative Optimum model, $F(1, 16) = 1.03$, $p > .25$; and 75.0% for the two-bumper tapping task, which was not significantly better than the Optimal Amplitude model, $F(1, 70) = 3.24$, $p > .05$, but significantly better than the Relative Optimum model, $F(1, 70) = 6.58$, $p < .025$. Part of the good fit of this model to the waving data is accomplished by the model's adoption of near-zero values for the preferred amplitude of the finger, and for the preferred frequency of the arm. While performance at these points may be optimal in a trivial sense (movement at zero amplitude or zero frequency requires no energy), these parameter values do not reflect the task requirements appropriately, since they predict that a subject instructed to move the finger or arm in the most comfortable manner would remain motionless.

In addition to considering the above modeling variations, we also evaluated one of the central assumptions of the virtual-oscillation hypothesis. We assumed that the collision of the fingertip with the bumper is elastic, so that stored energy contributes to the acceleration of the fingertip in the departure phase of each collision. What would happen if this assumption were violated? If the collision were inelastic, then less energy would be transferred between the fingertip and the bumper than is predicted by the assumption of elastic collision; similarly, if the energy transfer in each collision included some isometric contraction against the bumper, more energy would be transmitted than is predicted by the assumption of elastic collision. The assumption of inelastic collision reduced the goodness of fit of the models in every case. Similarly, the assumption that some of the energy transfer in each collision resulted from isometric exertion against the bumper

did not improve the fit of the Relative Optimum model significantly. (In this comparison, the relative contribution of elastic collision with the bumper and isometric contraction against it was estimated as a free parameter.) By contrast, allowing for some contribution of isometric pressure against the bumper increased the variance explained by the Optimal Amplitude model from 66.9% to 68.7%, $F(1, 76) = 4.371$, $p < .05$; and increased the variance explained by the Relative Optimum model from 60.9% to 64.9%, $F(1, 75) = 8.547$, $p < .005$.

As was discussed above, there are a number of different alternative models that in some respects do as well as the optimal-selection models. This is to be expected, because most of these alternative models incorporate some representation of both the frequency of movement and the virtual amplitude of movement. However, we believe that the two models we have focussed on are preferable for three reasons: (1) each has a clear theoretical rationale; (2) the pattern of optimal parameter values is similar across experiments; and (3) each is relatively insensitive to specific parameter values. Given the similarities between the two models, is it possible to say which is better? Perhaps further empirical work will be able to do so definitively. For now, the Optimal Amplitude model appears to have several advantages over the Relative Optimum model. It provides an equally good fit to the tapping data with one less free parameter, it is less sensitive to specific parameter values, and it proposes a specific mechanism by which the limb may produce oscillation at a full range of frequencies.

General discussion

We have found that the way subjects divide the work of displacing the fingertip among the finger, hand, and arm, in both unobstructed waving and in tapping, is consistent with the biomechanical properties of the individual segments. In all three tasks studied in our laboratory – in unobstructed waving (Rosenbaum et al., 1991) and in tapping against one or two bumpers (Experiments 1 and 2), the finger contributed most when fast, low-amplitude movements were required, whereas the arm contributed most when slow, high-amplitude movements were required. Subjects selected movements that reflected the optimal performance characteristics of each segment, as is assumed in the Optimal Selection model. Outside the laboratory, people do the same. For example, Michael Tree, violist of the Guarneri Quartet, reported, "I'll use a finger vibrato if I want it to be fast and narrow, producing an intense, glistening sound. But I'll use more wrist, and eventually more arm, if I want to find a fatter, more sensuous quality" (Blum, 1986, p. 42).

To apply the Optimal Selection model to our tapping tasks, we assumed that subjects controlled the impulse of collision by varying the virtual amplitude of oscillation. Moreover, studies of performance in other contexts also support the virtual-amplitude idea. For example, karate experts are trained to aim their blows past the impact surface (Feld, McNair, & Wilk, 1979). Conrad and Brooks (1974) trained monkeys to move a handle repeatedly through a 90° arc to hit two stops as rapidly as possible. When the range of movement was unexpectedly reduced to 60° or 30°, the monkeys held the handle against the stop for the same length of time as they otherwise would have spent completing the remainder of the unobstructed movement. The preservation of timing in interrupted oscillation is consistent with the notion that tapping against a barrier is treated as an oscillation through the barrier. We would expect that if the complementary experiment were conducted, in which an expected barrier to tapping was unexpectedly removed, the complementary result would be obtained. The greater the impulse of collision to be imparted, the farther the arm would travel past the bumper's anticipated position. In fact, such an *overshoot* phenomenon is familiar to anyone who has prepared to push open a door, only to find at the last moment that the door has been pulled open by someone on the other side.

In much the same vein, Asatryan and Feldman (1965) conducted classic experiments in which subjects first pulled against a spring and then did not correct for the displacement of the limb that occurred when the spring was released. The endpoints to which the arm travelled increased with the tension that was exerted. Asatryan and Feldman's task involved isometric muscle contraction, whereas we have been discussing isotonic (distance-covering) performance. Nonetheless, the similarity between Asatryan and Feldman's (1965) result and our identification of impulse of collision with amplitude is close.

When more or less forceful tapping was required, subjects in our experiment apparently varied their performance by modulating the amplitude of their movements. They hit the bumper differently by oscillating over different amplitudes, as was directly observed in the one-bumper experiment, and inferred from dwell times in the two-bumper experiment. Similarly, Keele, Ivry, and Pokorny (1987) reported that the contact duration of accented taps is longer than that of unaccented taps, in accordance with a virtual-amplitude interpretation (although we did not observe significant dwell-time variation as a function of impulse amplitude in our Experiment 1).

Modulation of the velocity of collision by change in the amplitude of movements was not, however, sufficient to account for all of the variation in performance. For example, in the one-bumper experiment, the required impulse of collision varied by more than a factor of 6 from the soft to the hard impulse conditions, but the velocity of the fingertip at the instant of collision varied by less than a factor of 3. This difference

reinforces the observation that subjects must also have changed the effective mass with which the bumper was struck, as is demonstrated, in fact, by the changes in the relative contribution of the three limb segments. Subjects may, of course, have deliberately recruited effectors of larger mass to get larger impulse amplitudes. However, such deliberate planning may have been unnecessary. The shift to larger effectors may have come about as an automatic consequence of the selection of larger virtual amplitudes, as is assumed in the two versions of the Optimal Selection model presented here.

Focussing now on the two model versions, we note that both have strengths and weaknesses. The Relative Optimum model is based on the direct evaluation of overall optimum performance of each segment, whereas the Optimal Amplitude model provides a mechanism for varying the stiffness of each joint, and thus its resonant frequency. The Relative Optimum model produced a better fit to the finger-waving data of Rosenbaum et al. (1991) than did the Optimal Amplitude model. However, the two models were statistically equivalent in accounting for movement selection in the tapping experiments, the amplitudes of the backswing in the one-bumper tapping experiment, and the dwell times in the two-bumper tapping experiment. Thus, we cannot distinguish between the models solely on the basis of their goodness of fit to the data, although the Optimal Amplitude model needs one fewer free parameter than the Relative Optimum model and therefore may be preferable on grounds of parsimony.

Promising as the two models are (the Optimal Amplitude model in particular), it remains true that neither of the two optimal selection models accounts spectacularly for all aspects of the observed performance. There are several reasons why this may be. First, we assumed, in the computation of the virtual amplitudes in the various conditions, that the underlying oscillation is sinusoidal, and that the collision with the bumper is perfectly elastic. These two assumptions have the twin virtues of parsimony (they provide a simple model of oscillation and collision) and tractability (the required virtual amplitudes are easily calculable). However, it may be that fingertip oscillation is represented better by a more complex model of oscillation, such as that proposed for the wrist by Kay et al. (1987). Second, sequential effects may have entered into our subjects' performance. When subjects draw lines of gradually increasing or gradually decreasing lengths, there is hysteresis in the selection of limb segments (Meulenbroek, Rosenbaum, Thomassen, & Schomaker, 1993). Similarly, if subjects adopt a particular manner of tapping at high rates, they may tend to maintain that pattern when they switch to an intermediate rate, but they may use another pattern at the intermediate rate if they switch to it from a slower rate (Boak, 1989). Although we attempted to eliminate sequential effects by having subjects execute each task once for practice before performing it for data collection, we may not have succeeded in eliminating this source of variation. Third, the models attempt to explain the one- and two-bumper tapping data with estimates of optimal performance obtained from different subjects in a different task. Fitting data from individually observed optimal-performance functions, or restricting the performance to be modeled to a narrower range, would presumably provide better overall fits. More important, however, is the fact that the tasks that are modeled comprise a very broad range of performance, from gentle finger waving to forceful tapping against a bumper. The demonstration of the models' general success in this broad domain of tasks suggests that the models are not restricted to a particular type of performance. Finally, the assumptions of the models may not have been fully met in all experimental conditions. To take one example, when required performance is very different from the optimum, such as hard tapping at very low rates, energy stored for recoil may contribute less to the performance, or isometric contraction may contribute more, and so there may be changes in the overall kinematics of movement, in violation of the models' assumptions.

These difficulties notwithstanding, one distinctly appealing feature of the virtual-oscillation hypothesis is that it allows a kinetic variable (impulse of collision) to be expressed in terms of a spatial variable (virtual amplitude). Reducing the number of variables to be controlled is one of the key ways to solve the degrees of freedom problem. That a force-related control variable may be represented spatially suggests that it may be possible to develop a unified conception of perceptual-motor performance and (spatial) cognition.

Acknowledgements Supported in part by NSF grants BNS 87-10933, BNS 90-08665 and SBR-9496290 (to DAR), an NIMH Research Scientist Award (to DAR), two NSF Research Opportunity awards (to DAR and JV), and the Hamilton College Faculty Research Fund (to JV). Frederick Diedrich is now at the Department of Psychology, Indiana University. Cathleen M. Moore is now at the Department of Psychology, Johns Hopkins University. We thank Brian Collett for advice, and for the hospitality of his laboratory in calibrating the apparatus. Comments by Thomas Carr, Caroline von Heugten, Herbert Heuer, Horst Krist, Loukia Loukopoulos, Tiffany Mattson, Claire Michaels, Douglas Weldon, and several anonymous reviewers helped us improve the paper.

References

Alexander, R. M. (1984). Elastic energy stores in running vertebrates. *American Zoologist, 24*, 85–94.

Asatryan, D. G., and Feldman, A. G. (1965). Functional tuning of the nervous system with control of movement or maintenance of a steady posture. 1. Mechanographic analysis of the work of the joint on execution of a postural task. *Biophysics, 10*, 925–935.

Barnes, H. J., Vaughan, J., Jorgensen, M. J., and Rosenbaum, D. A. (1989). A low-cost method for recording videotaped continuous movements with the Macintosh. *Behavior Research Methods, Instrumentation and Computers, 21*, 255–258.

Bernstein, N. (1967). *The coordination and regulation of movements.* London: Pergamon.

Bizzi, E., Hogan, N., Mussa-Ivaldi, F. A., and Giszter, S. (1992). Does the nervous system use equilibrium-point control to guide single and multiple joint movements? *Behavioral and Brain Sciences, 15,* 603–613.

Blum, D. (1986). *The art of quartet playing: The Guarneri Quartet in conversation with David Blum.* New York: Knopf.

Boak, J. (1989) Learning strategies within a constraint model of finger, hand, and arm movement. Undergraduate Honors' Thesis, Hamilton College Psychology Department.

Collard, R., and Povel, D.-J. (1982). Theory of serial pattern production: Tree traversals. *Psychological Review, 85,* 693–707.

Conrad, B., and Brooks, V. B. (1974). Effects of dentate cooling on rapid alternating arm movements. *Journal of Neurophysiology, 37,* 792–804.

Feld, M. S., McNair, R. E., and Wilk, S. R. (April, 1979). The physics of karate. *Scientific American, 240,* 150–158.

Feldman, A. G. (1980). Superposition of motor programs: I. Rhythmic forearm movements in man. *Neuroscience, 5,* 81–90.

Feynman, R. P., Leighton, R. B., and Sands, M. (1963). *The Feynman lectures on physics. Volume I.* Reading, MA: Addison–Wesley Publishing Co.

Hasan, Z. (1986). Optimized movement trajectories and joint stiffness in unperturbed, inertially loaded movements. *Biological Cybernetics, 53,* 373–382.

Hogan, N. (1985). The mechanics of multi-joint posture and movement control. *Biological Cybernetics, 52,* 315–331.

Hogan, N., and Flash, T. (1987). Moving gracefully: quantitative theories of motor coordination. *Trends in the Neurosciences, 10,* 170–174.

Holt, K. G., Hamill, J., and Andres, R. O. (1991). Predicting the minimal costs of human walking. *Medicine and Science of Sports and Exercise, 23,* 491–498.

Kay, B. A., Kelso, J. A. S., Saltzman, E. L., and Schöner, G. (1987). Space–time behavior of single and bimanual rhythmical movements: Data and limit cycle model. *Journal of Experimental Psychology: Human Perception and performance, 13,* 178–192.

Keele, S. W., Ivry, R. I., and Pokorny, R. A. (1987). Force control and its relation to timing. *Journal of Motor Behavior, 19,* 96–114.

Meulenbroek, R. G. J., Rosenbaum, D. A., Thomassen, A. J. W. M., and Schomaker, L. R. B. (1993). Limb-segment selection in drawing behavior. *Quarterly Journal of Experimental Psychology, 46,* 273–300.

Meyer, D. E., Abrams, R. A., Kornblum, S., Wright, C. E., and Smith, J. E. K. (1988). Optimality in human motor performance: Ideal control of rapid aimed movements. *Psychological Review, 95,* 340–370.

Mussa-Ivaldi, F. A., Hogan, N., and Bizzi, E. (1985). Neural, mechanical, and geometric factors subserving arm posture in humans. *Journal of Neuroscience, 5,* 2732–2743.

Myers, J. L., and Well, A. D. (1991). *Research design and statistical analysis.* New York: Harper-Collins Publishers.

Rosenbaum, D. A. (1991). *Human motor control.* San Diego: Academic Press.

Rosenbaum, D. A., Kenny, S., and Derr, M. A. (1983). Hierarchical control of rapid movement sequences. *Journal of Experimental Psychology: Human Perception and Performance, 9,* 86–102.

Rosenbaum, D. A., Slotta, J. D., Vaughan, J., and Plamondon, R. (1991). Optimal movement selection. *Psychological Science, 2,* 86–91.

Rumelhart, D. E., and McClelland, J. L. (1986). *Parallel distributed processing, Volume 1.* Cambridge: MIT Press.

Summers, J., Rosenbaum, D. A., Burns, B., and Ford, S. (1993). Production of polyrhythms. *Journal of Experimental Psychology: Human Perception and Performance, 19,* 416–428.

Vorberg, D., and Hambuch, R. (1978). On the temporal control of rhythmic performance. In J. Requin (Ed.), *Attention and performance VII.* Hillsdale, NJ: Erlbaum.

Wing, A. M. (1980). The long and short of timing in response sequences. In G. E. Stelmach & J. Requin (Eds.), *Tutorials in motor behavior* (pp. 469–486). Amsterdam: North-Holland.